

# Influence of Methyl Halide Treatment on Gold Nanoparticles Supported on Activated Carbon\*\*

Jacinto Sá, Alexandre Goguet, S. F. Rebecca Taylor, Ramchandra Tiruvalam, Christopher J. Kiely, Maarten Nachtegaal, Graham J. Hutchings, and Christopher Hardacre\*

The number of publications reporting the application of gold to catalytic processes has increased dramatically since the discovery in the 1980s<sup>[1,2]</sup> that supported nanoparticles of gold can be very active catalysts for industrially important reactions. Since then, gold has been found to be active for a large range of processes including hydrogenation reactions,<sup>[3]</sup> selective oxidations,<sup>[4]</sup> hydroaminations,<sup>[5]</sup> and epoxidations.<sup>[6]</sup> The applications reported range from environmental remediation<sup>[7]</sup> to the production of bulk and pharmaceutical chemicals.<sup>[8]</sup>

The performance of gold catalysts is closely related to the size of the deposited nanoparticles and the properties of the support used. Consequently, the preparation and stabilization aspects of Au nanoparticles are vital steps in the discovery of new and/or improved catalysts. However, the practical application of gold catalysts has often been limited because of low stability and irreversible deactivation during reaction and thermal pretreatment. Many studies have investigated the underlying causes behind the loss in activity and have reported surface poisoning, loss of metal–support interaction, and nanoparticle sintering as potential contributing factors. Reactivation of the catalysts is problematic, particularly in cases where the gold particles have increased in size, and, therefore, if it were possible to devise an effective method to redispersed the Au metal, this would be of significant benefit.

Redispersion of metals has been developed for platinum group metals (PGM) through the oxychlorination process.<sup>[9]</sup> This procedure requires temperatures above 500 °C and a series of reduction/oxidation treatments using chlorinated molecules such as 1,2-dichloropropane. However, depending on the end process in which these treated catalysts are to be used, this redispersion process can lead to further deactivation

by chlorine poisoning. The temperatures used in the oxychlorination approach can also limit its applicability because not all conventional supports are stable under the required treatment conditions.

Recently, Goguet et al.<sup>[10]</sup> demonstrated that large particles of gold (around 12–28 nm in size) supported on activated carbon (Au/C) can be dispersed down to atomic level during the carbonylation of methanol to methyl acetate in the presence of methyl iodide.<sup>[11]</sup> The dispersion of gold particles was attributed to the interaction of gold with the iodine. Although this is a remarkable transformation, the conditions utilized during the reaction are rather harsh (240 °C and 16 bar) and required a complex reaction mixture. This limits the general applicability of this method as a routine procedure for the dispersion of gold. Herein we show that gold dispersion is achievable under much milder conditions in terms of temperature and pressure using a simple CH<sub>3</sub>X/inert feed (X = Br or I) and the mechanism responsible of the dispersion is demonstrated.

Goguet et al. identified that the CH<sub>3</sub>I was the key species in the gold dispersion process.<sup>[10]</sup> To evaluate the influence of the presence of the reactants used in the carbonylation reaction mixture, and the impact of the process pressure, the possibility of achieving gold dispersion in the sole presence of CH<sub>3</sub>I at atmospheric pressure was evaluated. Figure 1 reports the X-ray diffraction (XRD) data recorded for the fresh Au/C and the same catalyst exposed for 1 h to a CH<sub>3</sub>I/N<sub>2</sub> mixture at 240 °C and atmospheric pressure. The Bragg reflections associated with Au(111) and (200) lattice planes, which were observable for the fresh catalyst, are essentially absent after exposure to CH<sub>3</sub>I/N<sub>2</sub> mixture at 240 °C for 1 h. A similar

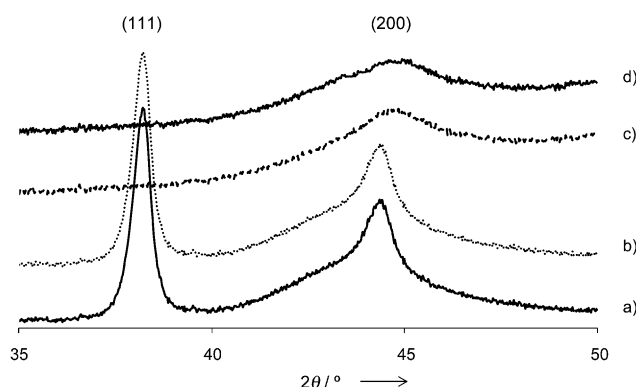


**Figure 1.** XRD patterns of gold supported on activated carbon a) fresh, after treatment with b) CH<sub>3</sub>Cl at 240 °C for 24 h, c) CH<sub>3</sub>I at 240 °C for 1 h, and d) CH<sub>3</sub>Br at 240 °C for 24 h.

[\*] Dr. J. Sá, Dr. A. Goguet, S. F. R. Taylor, Prof. C. Hardacre  
School of Chemistry and Chemical Engineering  
Queens University, Belfast, BT9 5AG (UK)  
E-mail: c.hardacre@qub.ac.uk

R. Tiruvalam, Prof. C. J. Kiely  
Department of Materials Science and Engineering  
Lehigh University, 5 East Packer Avenue  
Bethlehem, PA 18015-3195 (USA)

Dr. M. Nachtegaal  
Paul Scherrer Institute, 5232 Villigen PSI (Switzerland)

Prof. G. J. Hutchings  
Cardiff Catalysis Institute, School of Chemistry  
Cardiff University, CF10 3AT, Cardiff (UK)

[\*\*] We acknowledge the SLS for the provision of beam time and the EPSRC for a CASTech grant.

Supporting information for this article is available on the WWW under <http://dx.doi.org/10.1002/ange.201102066>.

effect was found when using  $\text{CH}_3\text{Br}$  (Figure 1). Interestingly, when a similar treatment was performed using  $\text{CH}_3\text{Cl}$  (or no methyl halide, see Figure S1 in the Supporting Information), the XRD pattern of the fresh catalyst remained unaffected even after 24 h of exposure. The different behavior of the alkyl halides may reflect the decrease in the C–X bond energy enabling the catalyst to activate the molecule. Importantly, the dispersion of the gold can be achieved in the sole presence of either  $\text{CH}_3\text{Br}$  or  $\text{CH}_3\text{I}$  at atmospheric pressure. Elemental analysis of the Au/C catalyst pre and post  $\text{CH}_3\text{I}$  or  $\text{CH}_3\text{Br}$  treatments indicated that no gold was lost through leaching during the process.

To evaluate more precisely the extent of the gold dispersion, high angle annular dark field (HAADF) imaging experiments were performed in an aberration-corrected scanning transmission electron microscope (STEM) on the fresh and  $\text{CH}_3\text{I}$  treated samples. Figure 2A shows that the fresh Au/C sample contained relatively large gold particles.

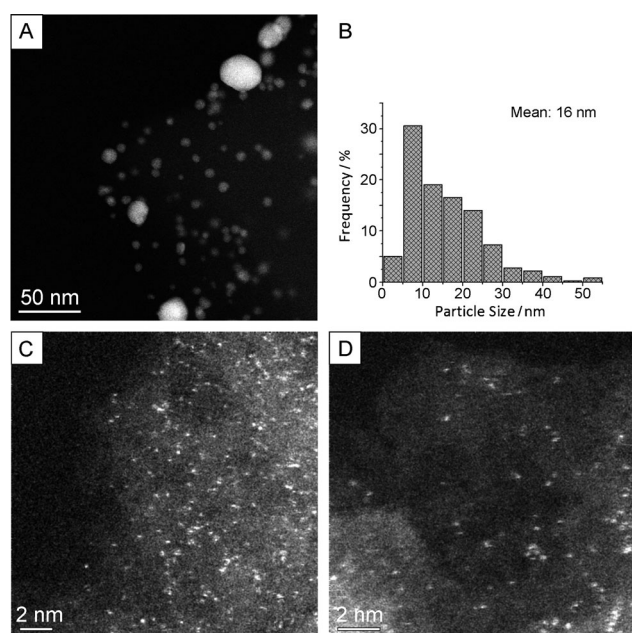
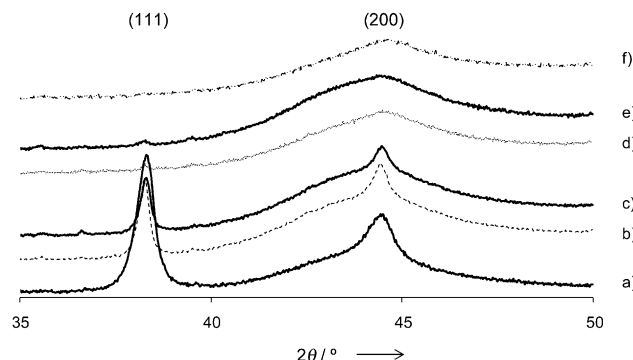


**Figure 2.** Influence of the  $\text{CH}_3\text{I}$  treatment on gold nanoparticles. A) HAADF-STEM image of gold supported on activated carbon untreated. B) Particle size distribution of starting Au/C material. C, D) HAADF-STEM of Au/C sample after  $\text{CH}_3\text{I}$  treatment at  $240^\circ\text{C}$  for 1 h. Some Au dimers and sub-nanometer Au clusters are also visible in (D).

The particle size distribution shown in Figure 2B, which was derived from analysis of multiple HAADF images, shows that the median Au particle size is about 16 nm. After the  $\text{CH}_3\text{I}$  treatment (Figure 2C,D), the gold was essentially distributed in the form of isolated Au atoms although a small number of Au dimers and sub-nanometer Au clusters are also observable. Closer inspection of the images obtained revealed the presence of some atoms having lower intensity than the other Au atoms. These features could potentially correspond to either lower atomic number iodine atoms or Au atoms which are at a different depth in the sample. Similar changes were

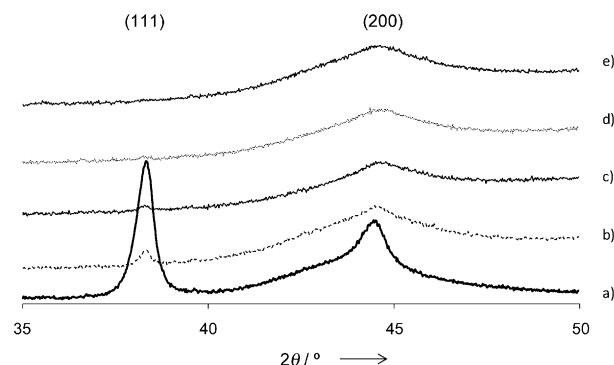
observed on exposing gold supported on graphite (Au/G) to  $\text{CH}_3\text{I}$  (see Figures S8 and S9 in the Supporting Information).

Figure 3 shows time-resolved XRD patterns obtained during a  $\text{CH}_3\text{I}$  treatment at  $240^\circ\text{C}$ . The results obtained



**Figure 3.** XRD patterns of gold supported on activated carbon a) untreated and after  $\text{CH}_3\text{I}$  treatment at  $240^\circ\text{C}$  for b) 1, c) 5, d) 15, e) 30, and f) 60 min.

showed that the diffraction peaks associated with gold decrease over a period of 5 min and only features associated with the carbon support were found after 15 min on stream indicating a rapid reaction. The influence of the process temperature was investigated to assess its impact on the dispersion kinetics. The diffraction patterns obtained after 1 h of exposure of the fresh catalyst at 50, 100, 150, and  $240^\circ\text{C}$  are presented in Figure 4. At all temperatures studied, a substantial decrease in the intensity of the gold diffraction peaks

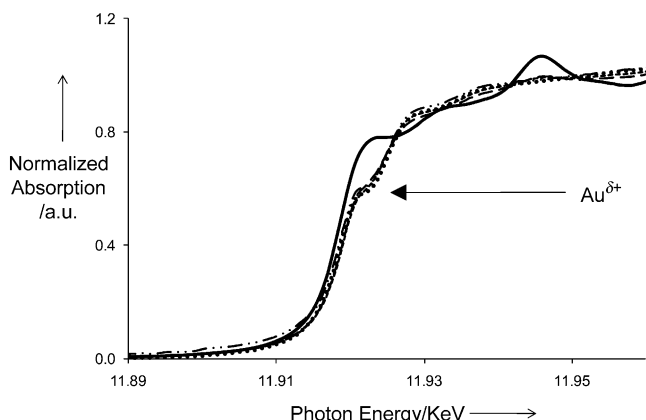


**Figure 4.** XRD patterns of gold supported on activated carbon a) untreated and after  $\text{CH}_3\text{I}$  treatment at b) 50, c) 100, d) 150, and e)  $240^\circ\text{C}$  for 1 h.

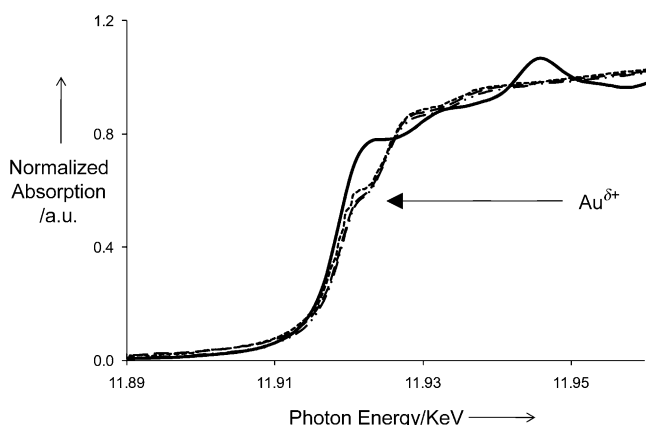
was observed. Increases in temperature did increase the rate of dispersion, as expected, with temperatures above  $100^\circ\text{C}$  being required to achieve complete disappearance of the Au(111) and (200) reflections after 1 h. The fact that such low temperatures may be employed suggests that only a low energy input is required to trigger dispersion of gold supported on activated carbon.

Table S1 in the Supporting Information reports the X-ray photoelectron spectroscopy (XPS) data obtained for the gold catalysts treated with  $\text{CH}_3\text{I}$  at temperatures between 50 and

240 °C. A slight increase of around 0.6 eV is observed in the Au 4f<sub>7/2</sub> feature following CH<sub>3</sub>I treatment. This suggests that the gold is associated with iodine as the binding energy of the Au 4f<sub>7/2</sub> feature (at 84.5 eV) is similar to that reported previously for AuI (84.6 eV).<sup>[12]</sup> This result is corroborated by the in situ X-ray absorption near-edge structure (XANES) recorded at the Au L<sub>III</sub> edge (Figures 5 and 6), where the appearance of a low intensity white line was detected for



**Figure 5.** XANES Au L<sub>III</sub> of gold supported on activated carbon untreated (—) and after CH<sub>3</sub>I treatment at 240 °C for 1 (···), 5 (---), 15 (----), and 30 min (- · -).



**Figure 6.** XANES Au L<sub>III</sub> of gold supported on activated carbon untreated (—) and after CH<sub>3</sub>I treatment at 50 (···), 150 (---), and 240 °C (----) for 1 h.

materials treated with CH<sub>3</sub>I. These findings are consistent with the data obtained during the carbonylation process which have been previously ascribed to the modification from bulk Au<sup>0</sup> to an oxidized form of gold (Au<sup>δ+</sup>).<sup>[10,12]</sup> It is also noticeable that a significant decrease in the Au 4f<sub>7/2</sub> feature occurs during the dispersion process which may be because of the presence of surface iodine causing shielding of the signal from the gold (see Figure S2 in the Supporting Information).<sup>[10]</sup>

Further analysis of the in situ Au L<sub>III</sub> extended X-ray absorption fine structure (EXAFS) data was performed to determine the average coordination number of neighbors

around the central gold atom. Table 1 and Table S2 as well as Figures S3 and S4 in the Supporting Information report the fitted structural parameters and the variation of the Au···Au

**Table 1:** Structural parameters from the fitted Au L<sub>III</sub> edge EXAFS spectra for the Au/C catalyst before and after CH<sub>3</sub>I treatments as a function of time and temperature.<sup>[a]</sup>

Temperature [°C]	Time [min]	Atom	Shell distance [Å]	Coordination number
50	60	Au	2.85	12.0
		Au	4.07	6.0
		I	2.54	2.1
		Au	2.81	1.9
100	60	I	2.54	2.4
150	60	I	2.56	3.0
240	60	I	2.55	3.0
240	1	I	2.54	1.6
240	5	Au	2.84	3.7
		I	2.53	1.7
		Au	2.84	2.3
240	15	I	2.55	2.8
240	30	I	2.54	2.1

[a] Full fitting parameters are summarized in Table S2 in the Supporting Information.

and Au···I coordination numbers obtained as a function of temperature and time on stream. The data from the untreated Au/C catalyst was fitted to gold having a coordination number of 12 at 2.85 Å, and 6 at 4.06 Å, corresponding to the first and second shell spacings in the bulk metal, respectively. For all CH<sub>3</sub>I treatment conditions, the coordination number around the central gold atom decreased from 12 to between 2 and 3 in agreement with the STEM data and a slight decrease in the nearest neighbor distance to around 2.75 Å was also found. This decrease in the Au···Au distance is also consistent with a decrease in the Au particle size. An additional feature at around 2.5 Å was also observed following CH<sub>3</sub>I treatment which is consistent with the Au–I bond length.<sup>[13]</sup>

From the XPS and XANES data it appears that the initial step of the dispersion mechanism involves the oxidation of surface gold atoms through an interaction with CH<sub>3</sub>I and the resulting formation of Au–I entities. The following stage, leading to the atomic dispersion of the large gold particles, could in principle proceed through two possible mechanisms, namely:

- 1) The large particles would undergo rupture because of the interaction of gold with iodine which results in its fragmentation into smaller particles with the process being repeated until an atomic dispersion is achieved.
- 2) The particle diameter would gradually shrink because of the progressive removal of Au–I entities from the surface of the particle.

Representative STEM-HAADF images obtained during increasing time on stream (i.e. increasing CH<sub>3</sub>I exposure) at 240 °C are shown in Figure S7 in the Supporting Information. After 1 min of contact time, the presence of intact (but smaller and fewer) Au particles, Au clusters on the nanometer scale and some isolated Au atoms were detected. With increased time on stream (5 min) the samples displayed

essentially gold clusters, dimers, and isolated atoms and the Au dispersion was near to completion. This behavior is consistent with the mechanism whereby the large particle diameters shrink and erode because of the progressive removal of Au–I entities from the main particles. The following reaction may be proposed for the transformation observed [Eq. (1)].



Dispersion of the supported gold by methyl iodide has a positive effect on the activity of these catalysts for methanol carbonylation as shown by large increase in activity during time on stream. However, the presence of halogen atoms on the surface of catalysts has been found to be detrimental in both non-gold<sup>[14]</sup> and gold-alloy systems.<sup>[15,16]</sup> To examine whether this process is a viable method to disperse gold for catalytic applications the treated catalysts were tested for the gas phase dehydrogenation of ethanol. This reaction has been extensively studied over a range of metal based catalysts<sup>[17–23]</sup> but only recently over gold.<sup>[24–27]</sup> Table 2 reports the catalytic

equivalent Au/C catalysts. Furthermore, unlike in the case of the treated Au/C catalysts, both the fresh and treated activated carbon supports produce ethanol as found for the untreated Au/C catalyst. The carbon, as well as the large gold particles, catalyze the dehydrogenation reaction and it is thought that the change in selectivity on CH<sub>3</sub>I treatment is due to the dispersion of the gold which then blocks the carbon sites for dehydrogenation. In addition, the reduction in the gold particle size also results in decreased dehydrogenation activity which is consistent with the observation that the optimum gold particle size for ethanol dehydrogenation has been found to be around 5 nm with a drastic decrease in activity as the particle size decreases.<sup>[27]</sup> These effects coupled together result in little dehydrogenation activity following CH<sub>3</sub>I treatment for the Au/C catalysts. Importantly, the Au/C catalyst is still much more active than the support even after the CH<sub>3</sub>I treatment which demonstrates that catalytic activity of the gold is still maintained, albeit lower than the fresh catalyst for this reaction. This decrease in activity is in contrast to the increased activity observed for the methanol carbonylation reaction. However, it is possible to reactivate

the catalysts following the CH<sub>3</sub>I by a combination of hydrothermal and reduction treatment at 190 °C for 15 min. For example, following CH<sub>3</sub>I treatment at 190 °C for 30 min, the activity of Au/G for the ethanol dehydrogenation reaction reduced from 13.5% to 8.6% conversion after 1 h on stream at 400 °C. Following treatment with H<sub>2</sub>O and hydrogen at 190 °C for 15 min the catalyst activity increased from 8.6 to 10.7% (Table 2).

The results reported here open up the possibility for reactivation and modification of gold-based catalysts for other reactions. In addition, it has been shown that individual gold atoms arranged as dimers can be effective catalysts, for example, in carbonylation reactions.

**Table 2:** Ethanol dehydrogenation catalytic performance at 400 °C after 1 h on stream for CH<sub>3</sub>I treated Au/C and Au/G catalysts.<sup>[a]</sup>

Catalyst	Temperature [°C]	Time [min]	Conversion [%]	Ethanal selectivity [%]	Methanal selectivity [%]	Ethene selectivity [%]
C	240	untreated	13.2	4	21	75
		30	4.4	2	34	64
	50	untreated	34.8	11	13	40
		60	19.3	0	32	68
		100	13.5	0	32	68
Au/C	150	60	13.7	0	28	72
	240	60	15.0	0	28	71
	240	1	13.3	0	29	71
	240	5	14.3	0	28	71
	240	15	13.9	0	30	70
G	240	30	18.2	0	26	74
		untreated	7.6	0	27	73
	190	30	6.9	0	26	74
		untreated	13.5	23	16	43
Au/G	190	30	8.6	13	22	64
		H <sub>2</sub> O + H <sub>2</sub>	10.7	9	24	66

[a] As a function of treatment time and temperature together with the effect of hydrothermal + reduction treatment at 190 °C for 15 min on the conversion for the Au/G catalyst. % Selectivity = 100 × yield/conversion.

performance at 400 °C in terms of conversion and selectivities for the various reaction products for the untreated and CH<sub>3</sub>I treated Au/C and Au/G catalysts.

Although the untreated Au/C catalyst was found to be the most active, all catalysts showed significant activity even after CH<sub>3</sub>I treatment. In addition, a substantial change in the product distribution was found following CH<sub>3</sub>I treatment with, in each case, the dehydrogenation to ethanal being completely suppressed and dehydration and reforming reactions dominating. Interestingly, the ratio for methanal/ethene is almost constant with respect to conversion. As shown the activated carbon support is also active but, in both the untreated and CH<sub>3</sub>I treated cases, is much less active than the

**Keywords:** carbon · dehydrogenation · gold · halides · nanoparticles

Received: March 23, 2011

Revised: June 26, 2011

Published online: August 10, 2011

- [1] M. Haruta, T. Kobayashi, H. Sano, N. Yamada, *Chem. Lett.* **1987**, 2, 405.
- [2] M. Haruta, *Nature* **2005**, 437, 1098.
- [3] for example, A. Corma, C. González-Arellano, M. Iglesias, F. Sánchez, *Appl. Catal. A* **2009**, 356, 99; D. A. Cadenhead, N. G. Masse, *J. Phys. Chem.* **1966**, 70, 3558; J. E. Bailie, G. J. Hutchings, *Chem. Commun.* **1999**, 2151.

- [4] for example, S. Biella, L. Prati, M. Rossi, *J. Catal.* **2002**, 206, 242; P. Landon, P. J. Collier, A. J. Papworth, C. J. Kiely, G. J. Hutchings, *Chem. Commun.* **2002**, 2058; S. Carrettin, P. McMorn, P. Johnston, K. Griffin, G. J. Hutchings, *Chem. Commun.* **2002**, 696; M. D. Hughes, Y. J. Xu, P. Jenkins, P. McMorn, P. Landon, D. I. Enache, A. F. Carley, G. A. Attard, G. J. Hutchings, F. King, E. H. Stitt, P. Johnston, K. Griffin, C. J. Kiely, *Nature* **2005**, 437, 1132.
- [5] A. Corma, P. Concepción, I. Domínguez, V. Fornés, M. J. Sabater, *J. Catal.* **2007**, 251, 39.
- [6] for example, T. Hayashi, K. Tanaka, M. Haruta, *J. Catal.* **1998**, 178, 56; A. K. Sinha, S. Seelan, S. Tsubota, M. Haruta, *Top. Catal.* **2004**, 29, 95; A. Corma, I. Domínguez, A. Doménech, V. Fornés, C. J. Gómez-García, T. Ródenas, M. J. Sabater, *J. Catal.* **2009**, 265, 238.
- [7] M. Magureanu, N. B. Mandache, J. Hu, R. Richards, M. Florea, V. I. Parvulescu, *Appl. Catal. B* **2007**, 76, 275.
- [8] C. W. Corti, R. J. Holliday, D. T. Thompson, *Appl. Catal. A* **2005**, 291, 253.
- [9] G. J. Arteaga, J. A. Anderson, S. M. Becker, C. H. Rochester, *J. Mol. Catal. A* **1999**, 145, 183, and references cited therein.
- [10] A. Goguet, C. Hardacre, I. Harvey, K. Narasimharao, Y. Saih, J. Sá, *J. Am. Chem. Soc.* **2009**, 131, 6973.
- [11] J. R. Zoeller, A. H. Singleton, G. C. Tustin, D. L. Carver, U.S. Pat. N° 6,506,933 and N° 6,509,293.
- [12] H. Kitagawa, N. Kojima, T. Nakajima, *J. Chem. Soc. Dalton Trans.* **1991**, 3121.
- [13] <http://crystals.ethz.ch/icsd/index.php>.
- [14] P. Gelin, M. Primet, *Appl. Catal. B* **2002**, 39, 1.
- [15] P. Broqvist, L. M. Molina, H. Gronbeck, B. Hammer, *J. Catal.* **2004**, 227, 217.
- [16] H.-S. Oh, J. H. Yang, C. K. Costello, Y. M. Wang, S. R. Bare, H. H. Kung, M. C. Kung, *J. Catal.* **2002**, 210, 375.
- [17] A. F. Lee, D. E. Gawthorpe, N. J. Hart, K. Wilson, *Surf. Sci.* **2004**, 548, 200.
- [18] M. K. Rajumon, M. W. Roberts, F. Wang, P. B. Wells, *J. Chem. Soc. Faraday Trans.* **1998**, 94, 3699.
- [19] E. Vesseli, A. Baraldi, G. Comelli, S. Lizzit, R. Rosei, *Chem-PhysChem* **2004**, 5, 113.
- [20] M. Bowker, R. P. Holroyd, R. G. Sharpe, J. S. Corneille, S. M. Francis, D. W. Goodman, *Surf. Sci.* **1997**, 370, 113.
- [21] J. L. Davis, M. A. Barteau, *Surf. Sci.* **1988**, 197, 123.
- [22] D. A. Chen, C. M. Friend, *J. Am. Chem. Soc.* **1998**, 120, 5017.
- [23] I. E. Wachs, R. J. Madix, *Appl. Surf. Sci.* **1978**, 1, 303.
- [24] C. Milone, R. Ingoglia, G. Neri, A. Pistone, G. Galvagno, *Appl. Catal. A* **2001**, 211, 251.
- [25] S. Biella, M. Rossi, *Chem. Commun.* **2003**, 378.
- [26] J. Gong, C. B. Mullins, *J. Am. Chem. Soc.* **2008**, 130, 16458.
- [27] Y. Guan, E. J. M. Hensen, *Appl. Catal. A* **2009**, 361, 49.